Velocity distributions and correlations in homogeneously heated granular media

Sung Joon Moon,* M. D. Shattuck,† and J. B. Swift
Center for Nonlinear Dynamics and Department of Physics, University of Texas, Austin, Texas 78712
(Received 27 April 2001; published 27 August 2001)

We compare the steady state velocity distributions from our three-dimensional inelastic hard sphere molecular dynamics simulation for homogeneously heated granular media, with the predictions of a mean field-type Enskog-Boltzmann equation for inelastic hard spheres [T. P. C. van Noije and M. H. Ernst, Granular Matter **1**, 57 (1998)]. Although we find qualitative agreement for all values of density and inelasticity, the quantitative disagreement approaches ~40% at high inelasticity or density. By contrast the predictions of the pseudo-Maxwell molecule model [J. A. Carrillo, C. Cercignani, and I. M. Gamba, Phys. Rev. E, **62**, 7700 (2000)] are both qualitatively and quantitatively different from those of our simulation. We also measure short-range and long-range velocity correlations exhibiting nonzero correlations at contact before the collision, and being consistent with a slow algebraic decay over a decade in the unit of the diameter of the particle, proportional to $r^{-(1+\alpha)}$, where $0.2<\alpha<0.3$. The existence of these correlations implies the failure of the molecular chaos assumption and the mean field approximation, which is responsible for the quantitative disagreement of the inelastic hard sphere kinetic theory.

DOI: 10.1103/PhysRevE.64.031303 PACS number(s): 45.70.−n, 05.20.Dd, 05.70.Ln

I. INTRODUCTION

Granular materials are collections of noncohesive macroscopic dissipative particles and are encountered in nature and in the industry [1]. These materials exhibit a wide variety of phenomena depending on the external forcing. The rapid granular flow regime, where the collisions are modeled as instantaneous binary inelastic collisions, is reminiscent of a gas of hard spheres. Thus, a common theoretical approach for this regime as a first order approximation is to model the system by means of the kinetic and the continuum equations for smooth inelastic hard spheres with a velocity-independent coefficient of restitution [2]. In the kinetic theory approach, the mean field-type Boltzmann or Enskog-Boltzmann equation for inelastic hard spheres is used, and most techniques are directly taken from the kinetic theory of a gas of elastic hard spheres [3]. It is known that this formulation is a reasonable description for nearly elastic ($1-e^2 \ll 1$, where e is the normal coefficient of restitution) and dilute cases. However, these theoretical models include approximations such as the truncation of series expansion or hierarchy, and the introduction of equation closure. The dissipative nature of the collision modifies the physics in a nontrivial way, and the accuracy and the limitation of the mean field-type kinetic description with these approximations is not yet known. The extension of the theory for the more inelastic and dense case, including surface friction, is one of major goals of the current inelastic kinetic theory [4].

There is an attractor in the phase space of the granular media, because inelastic collisions dissipate kinetic energy; in the absence of an external energy source, a granular medium loses its kinetic energy through collisions and becomes a static pile. To reach a steady state or an oscillatory state, a system of granular media requires an external energy source. In this paper, we investigate the steady state velocity distributions and velocity correlations of spatially homogeneous granular media subject to a volumetric Gaussian white noise forcing. This system has been studied by several authors [5,6,12,18] as a reference system for the kinetic theory of granular media. In this system, particles collide inelastically, and execute Brownian motion between collisions; the motion is analogous to Brownian dynamics of hard sphere suspension, but here the kinetic energy is dissipated due to the inelastic collisions rather than hydrodynamic drag. This system is far from equilibrium, and the steady state velocity distribution deviates from the Maxwell-Boltzmann (MB) distribution. The velocity distribution of this system was first theoretically studied by van Noije and Ernst [5], who obtained the approximate solutions to the inelastic hard sphere Enskog-Boltzmann equation with a Gaussian white noise forcing. Their results were tested against the direct simulation Monte Carlo (DSMC) method of the inelastic Enskog-Boltzmann equation [6], and a good agreement was found; it confirmed the accuracy of the approximate analysis of van Noije and Ernst, because the validity of the DSMC method relies on the validity of the inelastic Enskog-Boltzmann equation [7].

In the current study, we use a large molecular dynamics (MD) simulation (using up to 477 500 particles) of inelastic hard spheres to investigate the steady state velocity distributions, and quantitatively examine the accuracy of the inelastic Enskog-Boltzmann equation model for this system. Our method is free from the assumptions used in the inelastic kinetic theory, and it has an advantage that correlations can develop but has a disadvantage that it may have a finite simulation size effect.

We also compare our results with theoretical predictions of Carrillo *et al.* [8], who obtained the steady state velocity distribution by using the pseudo-Maxwell molecule model [9]. The Maxwell molecule model is the special case of the inverse power law model for the interparticle potential,

*Electronic address: moon@chaos.ph.utexas.edu
†Present address: Department of Physics, City College of CUNY, New York, NY 10031-9198.

whose potential has the form of $V(r) \sim r^{-4}$, where r is the interparticle distance. This model has been widely used for analytical studies as a reference system for more realistic systems, because the model facilitates calculations involving linearized Boltzmann operator. The pseudo-Maxwell molecule model is an inelastic analog of the Maxwell molecule model.

The remainder of the paper is organized as follows. Section II presents the method of the numerical simulation, and Sec. III briefly reviews the theoretical predictions of the inelastic hard sphere model and the pseudo-Maxwell molecule model. In Sec. IV, simulation results of the velocity distributions are presented, and these are compared with the theoretical predictions (Sec. IV A). The simulation results of the velocity correlations are also presented in this section (Sec. IV B). The paper is summarized and concluded in Sec. V.

II. NUMERICAL SIMULATION

We simulate an ensemble of inelastic hard sphere particles of diameter σ in a three-dimensional (3D) cubic box of each side 105.3σ, which are subject to a volumetric Gaussian white noise forcing. Particles obtain the kinetic energy from the white noise forcing, execute Brownian motion in between collisions, and dissipate the kinetic energy through inelastic collisions. To be consistent with the theoretical studies presented in Sec. III, we implement a velocity-independent coefficient of restitution e, and neglect the rotational degrees of freedom. We use an event-driven MD code originally developed to simulate the patterns in vertically oscillated granular layers. Excellent agreement was found between simulations and experiments [10]. We modify this code to implement the Gaussian white noise forcing. Brownian dynamics for hard sphere simulation was originated in the work of Ermak and McCammon [11], and the granular analog was introduced by Williams and MacKintosh [12] for their study of a one-dimensional system.

To implement Gaussian white noise forcing in our MD code, we start from a stochastic equation of motion for a particle. The equation of motion is given by

$$\ddot{x}_i(t) = \mathcal{F}_i^{(c)}(t) + \Gamma_i(t), \tag{1}$$

where the mass of the particle is the unity, x_i is the ith Cartesian component of the position, $\mathcal{F}_i^{(c)}$ is the ith component of the forcing due to the collisions, and $\Gamma_i(t)$ is the ith component of the stochastic forcing. The stochastic forcing term satisfies

$$\langle \Gamma_i(t) \rangle = 0, \tag{2}$$

which assures that the fluctuation cancels out on the average, where $\langle\rangle$ is an ensemble average, and

$$\langle \Gamma_i(t) \Gamma_j(t') \rangle = 2F \delta_{ij} \delta(t-t'), \tag{3}$$

where F is the strength of the correlation, δ_{ij} is the Kronecker delta, and $\delta(t)$ is the delta function. Equation (3) assures that the collisions well separated in time are statistically independent. We assume that all higher-order moments of the random variable $\Gamma_i(t)$ can be expressed in terms of the second moment, which is identical to the assumption that $\Gamma_i(t)$ is distributed according to the Gaussian distribution [13]. We implement an equation equivalent to Eq. (1) for each particle with a discrete time interval of a fixed size. It can be shown that the discrete Langevin equation for the velocity in between collisions subject to a Gaussian white noise is given by

$$v_i(t+\delta t) = v_i(t) + \sqrt{F}\sqrt{\delta t} G(0,1), \tag{4}$$

where F is the same quantity as in Eq. (3), δt is the time interval between the white noise forcing, and $G(0,1)$ is the unit Gaussian distribution random variable.

In the simulation, N_k particles are randomly chosen at every δt and are kicked in accordance with Eq. (4). To avoid the development of a mean flow in the system, particles to be kicked are randomly picked pairwise, and particles of this pair are kicked in opposite directions with the same speed to conserve the momentum. In an event-driven simulation, the random kickings are computationally expensive discrete events, because the collision list needs to be updated at each kicking. For the efficiency of the simulation, the mean kicking frequency needs to be minimized, or the mean kicking time for each particle $\overline{\delta t} (= \delta t N/N_k)$ needs to be maximized, where N is the total number of particles. We checked in the simulation that the velocity distributions do not change as far as $\overline{\delta t}$ is less than $1/(5\nu_{coll})$, where ν_{coll} is the mean collision frequency. We also checked that the velocity distributions do not depend on the choice of N_k and δt in these cases. Thus we keep $\overline{\delta t} \sim 1/(10\nu_{coll})$ throughout the simulations. The volume fraction ν varies from $\nu_o (= 4.29\%)$ to $5\nu_o$ $(= 21.4\%)$, which corresponds to 95 495 to 477 500 in the number of particles. Since the collisions are instantaneous, there is only one time scale determined by the granular temperature, $\sigma/\sqrt{T}$, where T is defined in Eq. (6). Therefore the temperature only rescales the time, and the results are independent of T. However, we fix the granular temperature at approximately the same value throughout the simulations. We prepare the initial conditions by locating particles in a regular lattice. We heat them, and wait until the transients decay away, ensuring that a steady state is reached. The data are taken periodically with a fixed time interval Δt. To assure that each data set is statistically uncorrelated, Δt is chosen larger than $5/\nu_{coll}$ in all cases, and $\Delta t \sim 10/\nu_{coll}$ in most cases. We obtain 50 such data sets for each simulation, and the error bars appearing in this paper are the standard deviations of these data sets. A periodic boundary condition is imposed in all directions.

III. REVIEW OF THEORY

In this section, we briefly review the results of the previous theoretical studies of van Noije and Ernst [5] and of Carrillo *et al.* [8]. Both studies are based on the mean field-type inelastic Enskog-Boltzmann equation.

Following standard procedures of the kinetic theory, it can be shown that the inelastic Enskog-Boltzmann equation for a system of spatially homogeneous granular particles subject

to a white noise forcing is given by

$$\frac{\partial f}{\partial t} = Q(f,f) + L_{FP} f, \tag{5}$$

where $f = f(\mathbf{c},t)$ is the single particle distribution function, $Q(f,f)$ is the collision operator, $\mathbf{c} = \mathbf{v}/\sqrt{2T(t)}$ is the velocity scaled by the characteristic velocity, and the mass is the unity. $T(t)$ is the granular temperature, defined as the variance of the velocity distribution per degree of freedom. For a 3D system,

$$T(t) = \frac{1}{3}\langle |\mathbf{v}(t) - \langle \mathbf{v}(t) \rangle|^2 \rangle. \tag{6}$$

The Fokker-Planck operator L_{FP} is a diffusion operator in the velocity space, which is given by

$$L_{FP} = F \boldsymbol{\nabla}_c^2, \tag{7}$$

where F is the strength of the correlation of Gaussian white noise stochastic forcing [defined in Eq. (3)], and $\boldsymbol{\nabla}_c^2$ is the Laplacian in the velocity space. The collision operator, $Q(f,f)$, is chosen depending on the interparticle potential model, and the most obvious one for the granular particles is the inelastic hard sphere collision operator.

van Noije and Ernst [5] obtained the steady state solutions to Eq. (5) using the inelastic hard sphere collision operator, and Carrillo *et al.* [8] obtained the steady state solutions using the pseudo-Maxwell collision operator. In both analyses, the Sonine polynomial expansion method was used to construct the solution. Sonine polynomials are associated Laguerre polynomials and have been used to construct solutions to the Boltzmann equation since Burnett [14] introduced them in the study of nonuniform gases. They are exact eigenfunctions of the linearized Boltzmann equation for Maxwell molecules. This expansion also leads to rapidly converging solutions of the linearized Boltzmann equation for other short-range repulsive potentials [3]. The Sonine polynomials of lower parameter 1/2 is defined by

$$S_{1/2}^{(n)}(x) = \sum_{p=0}^{n} \frac{\left(\frac{1}{2}+n\right)!}{\left(\frac{1}{2}+p\right)!(n-p)!p!}(-x)^p. \tag{8}$$

In the current study, c^2 is the argument of Sonine polynomials. The orthogonality relation with this argument is

$$\int_0^\infty c^2 e^{-c^2} S_{1/2}^{(n)}(c^2) S_{1/2}^{(m)}(c^2) dc = \frac{1}{2}\delta_{nm} \frac{\left(\frac{1}{2}+n\right)!}{n!}. \tag{9}$$

The first three Sonine polynomials are given by

$$S_{1/2}^{(0)}(c^2) = 1,$$

$$S_{1/2}^{(1)}(c^2) = \frac{3}{2} - c^2,$$

$$S_{1/2}^{(2)}(c^2) = \frac{15}{8} - \frac{5}{2}c^2 + \frac{1}{2}c^4.$$

For the inelastic hard sphere model, van Noije and Ernst [5] obtained the steady state solutions for 2D and 3D cases, by using the moment method [15], which was used in the analysis of the velocity distributions of homogeneously cooling of a freely evolving system. They expanded the solution in Sonine polynomials and neglected terms of higher order than the first nonvanishing correction to the MB distribution. The steady state solution for a 3D case, $f^s(c)$, is obtained as

$$f_{(HS)}^s(c) = f_{MB}(c)[1 + a_2^{HS} S_{1/2}^{(2)}(c^2)], \tag{10}$$

where

$$f_{MB}(c) = \frac{4}{\sqrt{\pi}} c^2 \exp(-c^2) \tag{11}$$

is the MB distribution (multiplied by an integration factor), and

$$a_2^{HS}(d,e) = \frac{16(1-e^2)(1-2e^2)}{73 + 56d - 24ed - 105e + 30(1-e)e^2}, \tag{12}$$

where d is the dimensionality of the system ($d=3$ in the current study), and HS stands for inelastic hard spheres.

For the pseudo-Maxwell molecule model, Carrillo *et al.* [8] obtained the steady state solution to Eq. (5) by doubly expanding the solution in the energy dissipation rate, $\epsilon = (1-e^2)/4$, and in Sonine polynomials. The deviation from the MB distribution was obtained up to the order of ϵ^4 [16]. The solution with the first nonvanishing correction to the MB distribution is of the order of ϵ^2, which is given by

$$f_{(MM)}^s(c) = f_{MB}(c)[1 + 4\epsilon^2 S_{1/2}^{(2)}(c^2)], \tag{13}$$

where MM stands for pseudo-Maxwell molecules. The first order deviations from the MB distribution in the two models have the same basis function $S_{1/2}^{(2)}(c^2)$, the second Sonine polynomial. We rewrite the normalized deviations from the MB in the two models as follows,

$$g^{HS}(e,c) = \frac{\Delta f^{HS}(e,c)}{f_{MB}(c)} = a_2^{HS}(e) S_{1/2}^{(2)}(c^2), \tag{14}$$

$$g^{MM}(e,c) = \frac{\Delta f^{MM}(e,c)}{f_{MB}(c)} = a_2^{MM}(e) S_{1/2}^{(2)}(c^2), \tag{15}$$

where

$$a_2^{MM}(e) = (1-e^2)^2/4 = 4\epsilon^2. \tag{16}$$

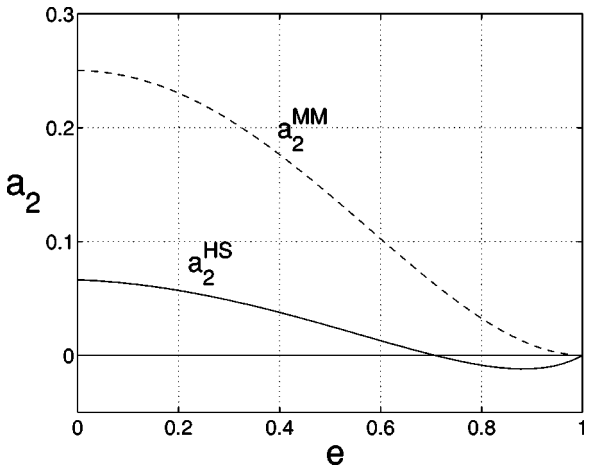

FIG. 1. The deviation from the MB distribution predicted by the theory a_2 as a function of the coefficient of restitution e. $a_2^{HS}(e)$ is the coefficient of the second Sonine polynomial from the inelastic hard sphere model, and $a_2^{MM}(e)$ is that from the pseudo-Maxwell molecule model.

The coefficients of the second Sonine polynomial for the two models, $a_2^{HS}(e)$ and $a_2^{MM}(e)$, are compared in Fig. 1.

To summarize, the predictions of the inelastic hard sphere model and those of the pseudo-Maxwell molecule model are different mainly in two ways.

(1) There is a crossover from positive to negative values in $a_2^{HS}(e)$ as e increases, and it is negative for $1/\sqrt{2}<e<1.0$, while $a_2^{MM}(e)$ is positive definite, $4\epsilon^2$. The high energy tail is always overpopulated in the pseudo-Maxwell molecule model, while it is underpopulated for $e>1/\sqrt{2}$ in the inelastic hard sphere model, when the series is truncated at this order.

(2) The deviation from the MB distribution in the pseudo-Maxwell molecule model is quantitatively much larger than that in the inelastic hard sphere model. Note that the analysis of the pseudo-Maxwell molecule model uses a small inelasticity assumption, while the analysis of the inelastic hard sphere model has no such assumption.

IV. SIMULATION RESULTS

A. Velocity distributions

We measure the velocity of each particle periodically in time with a fixed time interval of $\Delta t \sim 10/\nu_{coll}$, which is chosen to assure that each data set is statistically uncorrelated. The measured velocities are binned, and the bin size is $\Delta c = 0.1$. The velocity distributions for two coefficients of restitution, $e=0.1$ and $e=0.9$, are obtained in the simulation (Fig. 2). As in the inelastic hard sphere theory, high velocity tail is overpopulated for $e=0.1$, and slightly underpopulated for $e=0.9$, compared to the MB distribution.

We define the normalized deviation from the MB distribution $g(c)$, which is obtained in the simulation,

$$f^s_{(MD)}(c) = f_{MB}(c)[1+g(c)], \tag{17}$$

where the subscript (MD) means this is obtained in the MD

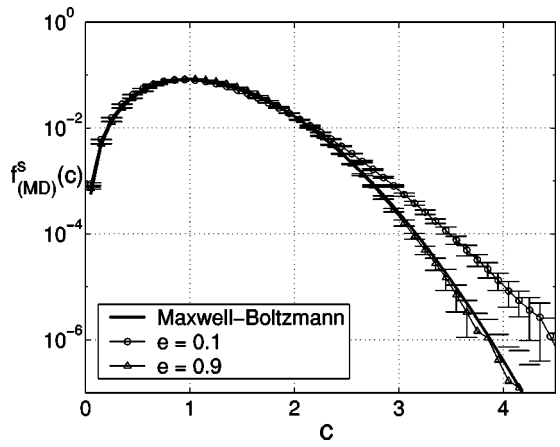

FIG. 2. The steady state velocity distributions $f^s_{(MD)}(c)$ obtained from the simulation for two coefficients of restitution, $e=0.1$ and $e=0.9$. The volume fraction is $5\nu_o$. The thick solid line is the MB distribution function.

simulation. Assuming $g(c)$ is a smooth function in the scale of $\Delta c(\ll 1)$, $g(c)$ can be approximated as

$$g\left(c_o+\frac{\Delta c}{2}\right) \approx \frac{\int_{c_o}^{c_o+\Delta c} f^s_{(MD)}(c)\,dc}{\int_{c_o}^{c_o+\Delta c} \frac{4}{\sqrt{\pi}} e^{-c^2} c^2\,dc} - 1. \tag{18}$$

The numerator in Eq. (18) is the total number of particles in the bin, which is a number counted in the simulation, and the denominator can be evaluated using the error function table. $g(c)$ calculated using Eq. (18) for the data in Fig. 2 is shown in Fig. 3. For direct comparison between our simulation results and the above theoretical predictions, we calculate the coefficient of the second Sonine polynomial a_2^{MD} from our measurements. As in the theoretical analyses, we assume $f^s_{(MD)}(c)$ is expanded in Sonine polynomials,

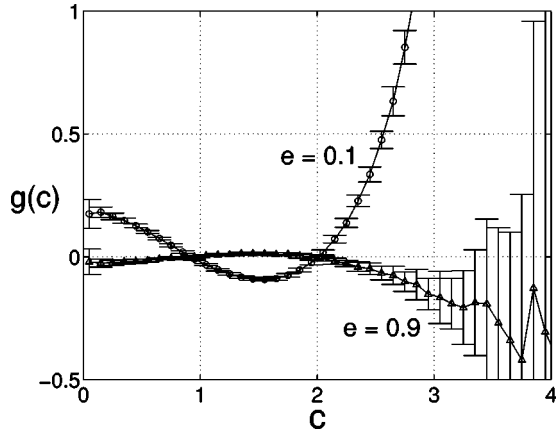

FIG. 3. The normalized deviation from the MB distribution $g(c)$ obtained from the simulation for two coefficients of restitution, $e=0.1$ and $e=0.9$. The volume fraction is $5\nu_o$. The error is large for $c>3$, because it involves division by a very small number.

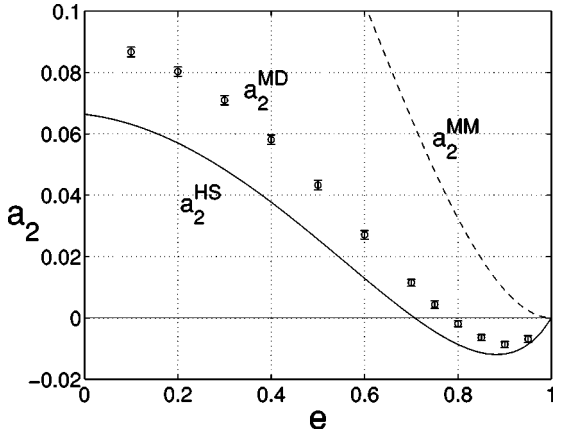

FIG. 4. A comparison of a_2's from the three models, the kinetic theory of the inelastic hard sphere model (solid curve), the kinetic theory of the pseudo-Maxwell molecule mode (dashed curve), and the MD simulation (open circles). The volume fraction is $5\nu_o$ for the simulation.

$$f^s_{(MD)}(c)=f_{MB}(c)\left[1+\sum_{k=2}^{\infty} a_k^{MD} S_{1/2}^{(k)}(c^2)\right], \tag{19}$$

where a_1^{MD} is not included, because it is identically zero in theory. We checked in the simulation that a_1^{MD} is less than 10^{-4} in all cases.

In the simulation, we can use either of the following two formulas to calculate a_k^{MD}, the coefficient of the kth Sonine polynomial. First, a_k^{MD}'s can be obtained from the following numerical integration, using the orthogonality relation for Sonine polynomials,

$$a_k^{MD}=\frac{2^k k!}{(2k+1)!!}\int_0^{\infty} f^s_{(MD)}(c) S_{1/2}^{(k)}(c^2)dc. \tag{20}$$

Second, we can make use of the recurrence relation of a_k^{MD}'s. Starting from the definition of Sonine polynomials, Eq. (8), it can be shown that for $k>2$, a_k^{MD} satisfies

$$a_k^{MD}=\frac{(-1)^k 2^k}{(2k+1)!!}\langle c^{2k}\rangle+(-1)^{k+1}+\sum_{p=1}^{k-2}(-1)^{p+1}\binom{k}{p} a_{k-p}^{MD}, \tag{21}$$

where $\langle c^{2k}\rangle$ is the $2k$th moment. It is straightforward to numerically evaluate the integration in both formulas. The above two relations, Eqs. (20) and (21), are mathematically identical. However, the errors of the lower k coefficients are accumulated on higher k coefficients in Eq. (21), while each a_k^{MD} is determined independently in Eq. (20). The results obtained using Eqs. (20) and (21) are nearly the same for small k, and they deviate more for larger k. a_2^{MD} is obtained using Eq. (20), which is compared with the theoretical predictions Eq. (12), a_2^{HS}, and Eq. (16), a_2^{MM} (Fig. 4). The simulation results deviate more from the predictions of the inelastic hard sphere kinetic theory as the system becomes more inelastic, and a_2^{MD} has a crossover between the positive and the negative values at around $e\sim 0.8$, while it was predicted to occur at $1/\sqrt{2}$ by the inelastic hard sphere theory. The pseudo-Maxwell molecule model does not predict a crossover behavior of a_2^{MM}, and the predictions of this model deviate quantitatively from the kinetic theory and simulations of the inelastic hard sphere model.

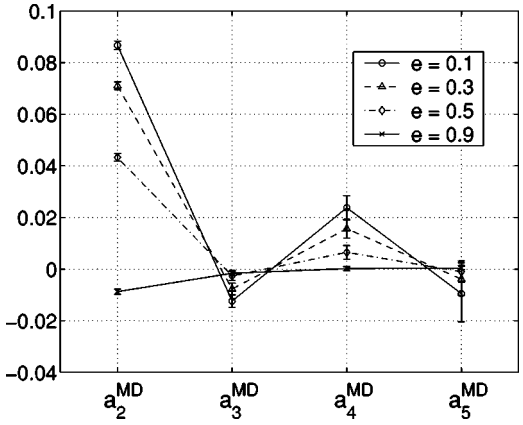

FIG. 5. The Sonine polynomial series converges slower as e decreases. The first four nonvanishing coefficients, from a_2^{MD} to a_5^{MD}, are calculated, which are obtained from the simulation for four coefficients of restitution. The volume fraction is $5\nu_o$.

In the simulation, all a_k^{MD}'s can be obtained by using Eq. (20). For larger k, the weight of the high velocity data exhibiting strong fluctuations become larger, and so does the uncertainty of a_k^{MD}. We calculate up to a_5^{MD} for various coefficients of restitution (Fig. 5). For nearly elastic case, for instance $e=0.9$, the series converges rapidly as in many cases of elastic hard spheres. However, as the system becomes more inelastic, the series converges more slowly. For $e=0.1$, a_4^{MD} is about 30% of a_2^{MD}. It is shown that how the first few nonvanishing coefficients of the Sonine polynomial series obtained in the simulation affect the fitting (Fig. 6).

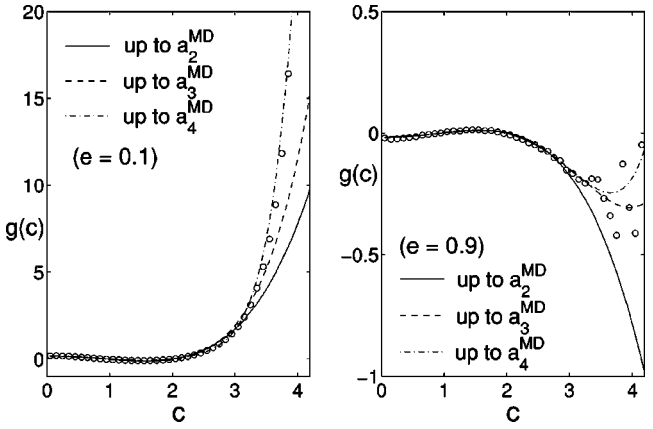

FIG. 6. The normalized deviations from the MB distribution $g(c)$, obtained in the simulation (open circles), are compared with the fitted curves using the coefficients of the Sonine polynomial expansion calculated using the simulation data, which are shown for two coefficients of restitution, $e=0.1$, and $e=0.9$. The terms are successively added to the Sonine polynomial expansion up to a_4^{MD}. The volume fraction is $5\nu_o$ for both, and the error bars for the data are not included for better comparison with fitting curves.

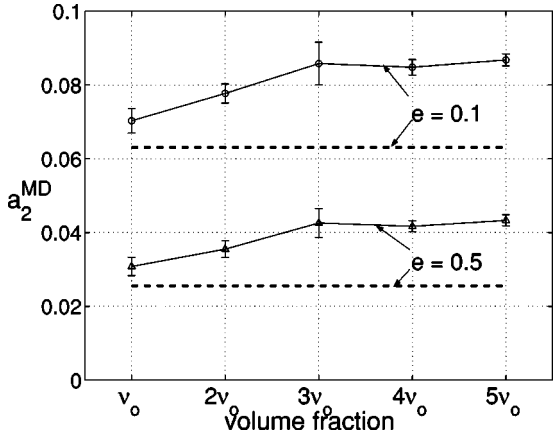

FIG. 7. The values of a_2^{MD} obtained in the simulation as a function of density for two coefficients of restitution, $e=0.1$ and $e=0.5$. Dashed lines are the predictions of the inelastic hard sphere kinetic theory, which do not depend on the density.

For $e=0.1$, a_2^{MD} fits the measured data well up to $v \sim 3\sqrt{2T} \sim 4\sqrt{T}$, but the high energy tail is fitted well only when the series are kept up to a_4^{MD}. For $e=0.9$, it shows the same tendency. When we fit the data only with a_2^{MD} in this case, $f^s_{(MD)}(c)$ becomes negative for $c>4.2$ and becomes negative infinity as c goes to infinity. Such nonphysical behavior disappears when we include a_3^{MD}.

In the theoretical predictions, the steady state velocity distribution and a_2^{HS} do not depend on the density, and it is a function of the coefficient of restitution and the dimensionality only. However, we find that it also depends on the density (Fig. 7). The value of a_2^{MD} decreases as the system becomes more dilute. For the smallest volume fraction we used ν_o the value of a_2^{MD} deviates by only few percent from the predictions of the inelastic hard sphere theory. We plot a_4^{MD}'s for various densities in Fig. 8 (a_3^{MD}'s are very small, as shown in Fig. 5). It follows the same tendency as a_2^{MD} does; as the system becomes denser, a_4^{MD} gets larger.

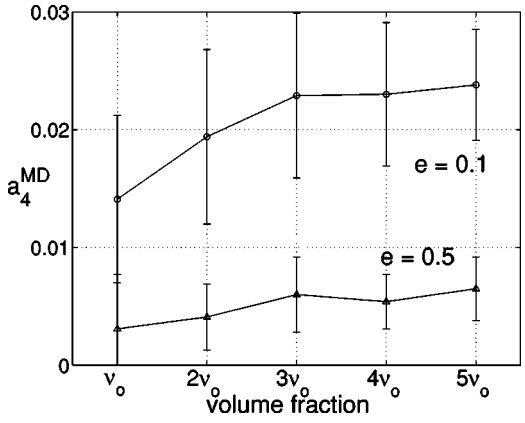

FIG. 8. The density dependence of a_4^{MD} for two coefficients of restitution, $e=0.1$ and $e=0.5$, obtained in the simulation. Predictions are not available, because they have not been calculated in the theoretical studies. Error bars for these data are bigger than those for a_2^{MD} (Fig. 7), because in calculating a_4^{MD} higher velocity data have more weight exhibiting stronger fluctuations.

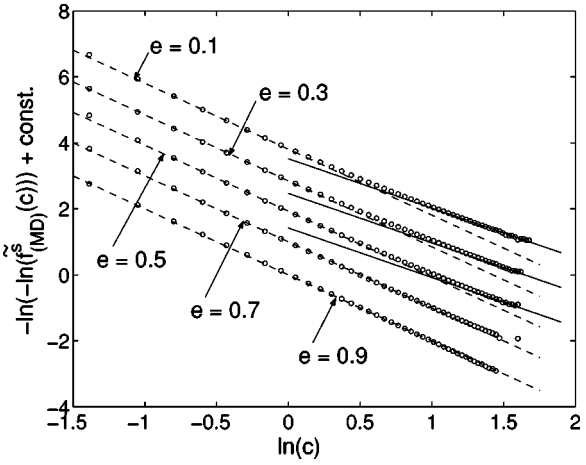

FIG. 9. A crossover behavior of the velocity distribution function $\tilde{f}^s_{(MD)}(c)$ (open circles) from $\sim\exp(-\mathcal{A}c^2)$ (compared with dashed lines) to $\sim\exp(-\mathcal{A}'c^{3/2})$ (compared with solid lines) is observed for higher inelasticities ($e<0.5$). The volume fraction is $5\nu_o$, and $\mathcal{A}$ and $\mathcal{A}'$ are arbitrary constants.

Finally, we examine the asymptotic behavior of the high energy tails of the velocity distribution functions. van Noije and Ernst [5] found for this system that a high energy tail shows an asymptotic behavior $\sim\exp(-\mathcal{A}'c^{3/2})$. We measure the velocity distribution function $\tilde{f}^s_{(MD)}(c)$, which is defined as

$$1 = \int \tilde{f}^s_{(MD)}(c)\,d\mathbf{c} = \int \tilde{f}^s_{(MD)}(c)\,4\pi c^2 dc = \int f^s_{(MD)}(c)\,dc. \tag{22}$$

To investigate the power of the argument of the exponential function, we renormalize $\tilde{f}^s_{(MD)}(c)$ with its maximum value. We observe the crossover behavior from $\sim\exp(-\mathcal{A}c^2)$ to $\sim\exp(-\mathcal{A}'c^{3/2})$ as c increases, for $e\leqslant 0.5$ (Fig. 9).

B. Velocity correlations

Two major approximations imposed in the kinetic theory discussed in Sec. III are the mean field approximation and the truncation of the hierarchy by introducing the molecular chaos assumption. In this section, we examine the validity of each of the above approximations for this system by quantitatively investigating the parallel velocity correlations, in long range and short range, respectively. It is known that a system of granular media exhibits strong spatial correlations [12,17,18], such as velocity correlations, but there is still the lack of a quantitative study of a 3D system. We suggest that the deviation of a_2^{MD} from a_2^{HS} originates from the failure of the above approximations.

We define the parallel velocity correlation function as

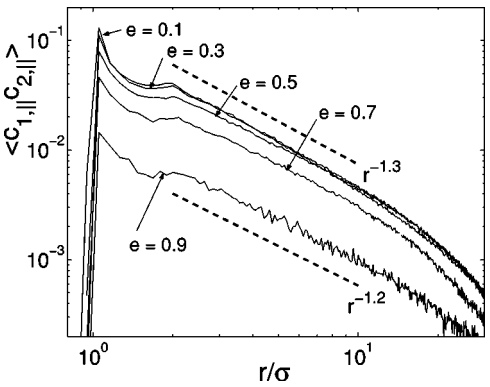

FIG. 10. The parallel velocity correlations for various coefficients of restitution. The volume fraction is $5\nu_o$. Dashed lines are the curves following the power law, which are included for comparison. The curves deviate from the power law for $r/\sigma>20$, because of the finite system size effect. Error bars are not shown for clarity.

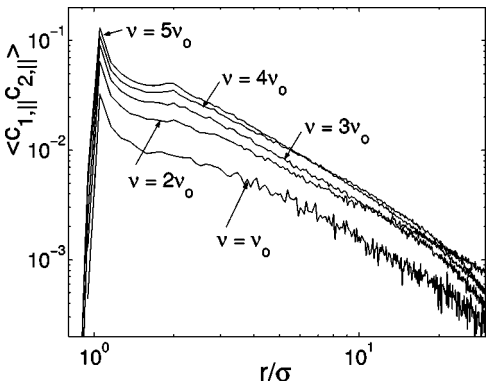

FIG. 11. The parallel velocity correlations for various densities. The coefficient of restitution is 0.1. They have the same tendency for other coefficients of restitution (not shown here).

$$\langle c_{1,||}c_{2,||}\rangle=\frac{1}{N}\int\langle\mathbf{c}(\mathbf{r}+\mathbf{r}')\cdot\hat{\mathbf{r}}\rho(\mathbf{r}+\mathbf{r}')\mathbf{c}(\mathbf{r}')\cdot\hat{\mathbf{r}}\rho(\mathbf{r}')\rangle d\mathbf{r}', \tag{23}$$

where $\hat{\mathbf{r}}=\mathbf{r}/|\mathbf{r}|$, and $\rho(\mathbf{r})$ is the local particle density,

$$\rho(\mathbf{r})=\sum_{i=1}^{N}\delta(\mathbf{r}-\mathbf{r}_i). \tag{24}$$

We approximately evaluate this quantity using the following formula,

$$\langle c_{1,||}c_{2,||}\rangle=\sum\frac{c_{1,||}c_{2,||}}{N_r}, \tag{25}$$

where the parallel direction is along the line of centers of the particle pair under consideration, N_r is the number of particles in a shell of thickness δr and inner radius r, and the summation is done over N_r. We use $\delta r=0.1053\sigma$.

1. Long-range correlations

The parallel velocity correlations are obtained by averaging over 50 statistically uncorrelated data sets. We calculate those for various coefficients of restitution as a function of dimensionless distance r/σ (Fig. 10), and for various densities (Fig. 11). The data are shown only for $r/\sigma<30$, because they are subject to the finite system size effect for larger r/σ. The parallel velocity correlations in our simulation are consistent with slow algebraic decay over a decade, $\sim r^{-(1+\delta)}$, where $0.2<\delta<0.3$. This behavior is close to the theoretical prediction of van Noije *et al.* [18], who predicted the r^{-1} power law from the mode coupling theory. The correlations in our simulation get stronger for more inelastic or more dense system, which implies that the mean field approximation is reliable only for nearly elastic and dilute cases.

2. Short-range correlations

In this section, we investigate the velocity correlations at contact before the collision, to examine the validity of the molecular chaos assumption. A nonzero value of these correlations is the signature of the failure of the molecular chaos assumption; the velocities are more ''parallelized'' after the collision, since only the normal component of relative velocity of colliding particles are reduced at the collision, which means that if the velocities are already parallelized before the collision, it would indicate that the colliding pair have ''memory'' on the collisions in the past, and they are correlated. We find that for high inelasticity and density, the precollisional parallel velocity correlation value reaches up to $\sim$15% of the temperature. Even for dilute or nearly elastic cases, these are not negligibly small.

We calculate the velocity correlations of precollisional and postcollisional states by evaluating Eq. (25) for approaching ($\mathbf{r}_{12}\cdot\mathbf{c}_{12}<0$) and separating particles ($\mathbf{r}_{12}\cdot\mathbf{c}_{12}>0$), respectively, where $\mathbf{x}_{12}=\mathbf{x}_1-\mathbf{x}_2$ for $\mathbf{x}=\mathbf{r}$ or $\mathbf{c}$. We calculate the precollisional state of short-range ($1<r/\sigma<2$) parallel velocity correlations (Fig. 12), and their postcollisional state (Fig. 13), for various coefficients of restitution. The values of the precollisional correlations are not negli-

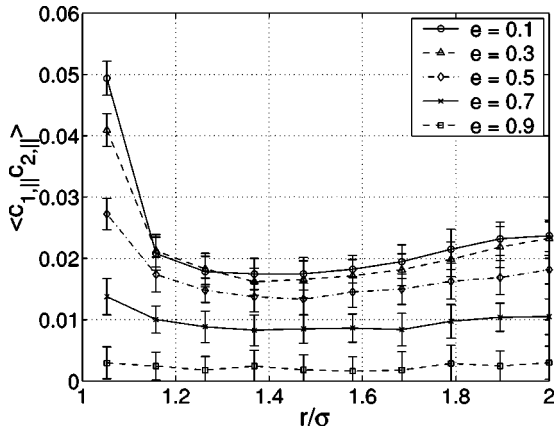

FIG. 12. The short-range precollisional parallel velocity correlations for various coefficients of restitution. The volume fraction is $5\nu_o$.

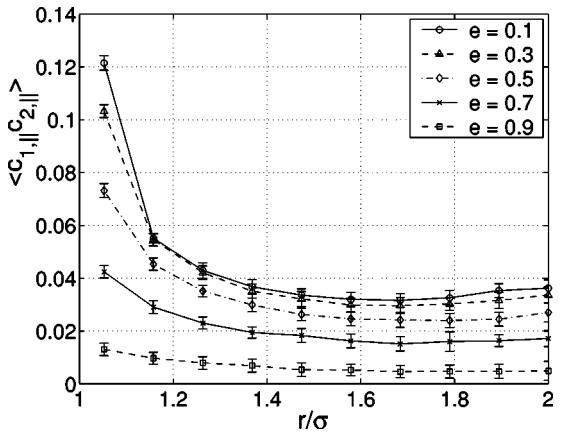

FIG. 13. The short-range postcollisional parallel velocity correlations for various coefficients of restitution. The volume fraction is $5\nu_o$.

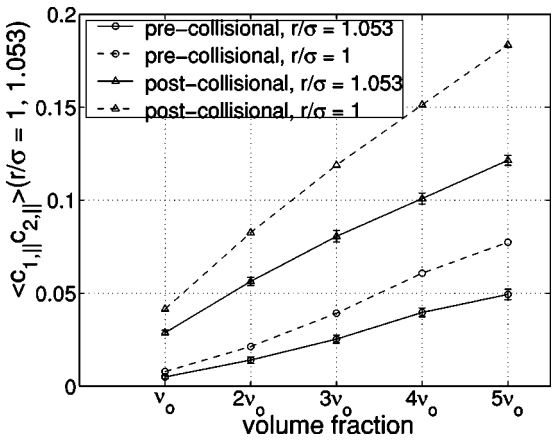

FIG. 15. The precollisional and postcollisional parallel velocity correlations at $r/\sigma=1.053$ (solid lines) and estimated values at contact, $r/\sigma=1$ (dashed lines), as a function of the density. The coefficient of restitution is 0.1.

gible compared to the temperature of the system. Postcollisional correlations are more than twice as large as precollisional correlations.

The maximum values of the velocity correlations in Figs. 12 and 13 are not the values at the contact, $r=\sigma$, because of the finite size of the bins in the measurements; instead, those are values at $r/\sigma=1.053$. The values at $r=\sigma$ are estimated by extrapolating the data in the interval $1<r/\sigma<2$ using the least square fit with fifth-order polynomials. We estimate the velocity correlations at contact, $r=\sigma$, as a function of the coefficient of restitution (Fig. 14), and as a function of the density (Fig. 15). Since the velocity correlation varies rapidly as r/σ decreases to 1, these estimations may be regarded only as approximate lower bounds. The velocity correlations at contact in this system show almost linear behavior both in density and the coefficient of restitution.

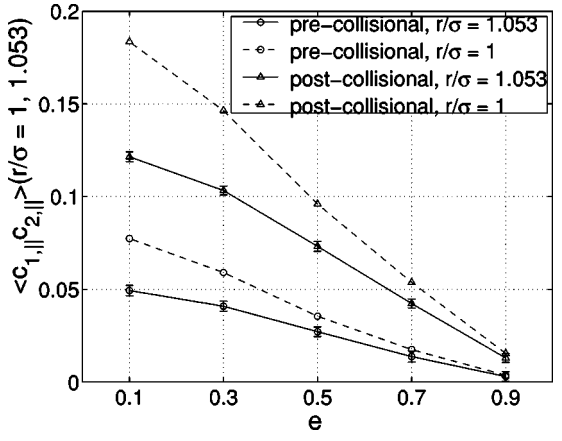

FIG. 14. The precollisional and postcollisional parallel velocity correlations at $r/\sigma=1.053$ (solid lines) and estimated values at contact, $r/\sigma=1$ (dashed lines), as a function of the coefficient of restitution. The volume fraction is $5\nu_o$. The values at contact are obtained by extrapolating the data in Figs. 12 and 13, using fifth-order polynomials. These are extrapolated values from the average values, and the error bars are not systematically determined. The error may be of the same order as the values at $r/\sigma=1.053$ in Figs. 12 and 13.

V. DISCUSSION

We have investigated the velocity distributions and parallel velocity correlations of $3D$ homogeneously heated granular media for various densities and inelasticities, using an inelastic hard sphere MD simulation. The deviations from the MB distribution in our simulations qualitatively agree with the results of the mean field-type inelastic hard sphere kinetic theory [5], but we found that there is systematic quantitative difference.

We observed the high energy tails are consistent with $\sim\exp(-\mathcal{A}'c^{3/2})$ for $e\leqslant 0.5$, but not for others. Since the elastic case ($e=1.0$) has no crossover from $\sim\exp(-\mathcal{A}c^2)$ to $\sim\exp(-\mathcal{A}'c^{3/2})$, we expect that this crossover behavior may occur at higher velocities as e approaches to 1.0, if it occurs. However, we were not able to check whether the crossover occurs for $e>0.5$ or never occurs, because our system is finite. It is interesting to note that the same behavior was experimentally observed in a system with different forcing mechanism [19].

We found that the steady state velocity distributions in the simulation depend on the density as well as the coefficient of restitution, while they depend only on the latter in the theory. The discrepancy between our simulation results and the theoretical predictions increases as the system becomes more inelastic or more dense, and the quantitative disagreement reaches up to $\sim 40\%$. This behavior is consistent with the results of van Noije and co-workers [18,20], who found that the collision frequency measured in a $2D$ MD simulation deviates more from the predictions of the inelastic Enskog-Boltzmann equation as the system becomes more inelastic. We suggest that the disagreement originates from the failure of two major approximations in the theory, the mean field approximation and the molecular chaos assumption. To examine the accuracy and the limitation of these approximations, we quantitatively investigated the parallel velocity correlations of this system.

We found that the long-range parallel velocity correlations are consistent with a slow algebraic decay, $\sim r^{-(1+\delta)}$, where $0.2<\delta<0.3$. This result is close to the theoretical predictions of van Noije *et al.* [18], who renormalized various quantities such as the collision frequency using the mode coupling theory and predicted r^{-1} power law for velocity correlations in the system we studied. Because of these strong correlations, the mean field approximation is not a good one unless the system is nearly elastic or very dilute.

We also found that the velocity correlations at contact before the collision are not negligible. We measured the short-range velocity correlations of precollisional and postcollisional states separately to examine the validity of the molecular chaos assumption. The precollisional correlations at contact are about a half of the postcollisional correlations. The correlations at contact are almost linearly proportional to both the density and the coefficient of restitution, which is consistent with the recent results of Soto and Mareschal [21], who studied the velocity correlations of a $2D$ homogeneously cooling granular media in nearly elastic regime.

We also examined the convergence of the Sonine polynomial expansion technique used in the inelastic kinetic theory, and found that the series converges more slowly as the system becomes more inelastic.

Finally, we compared the steady state velocity distributions in the simulations with the theoretical predictions of Carrillo *et al.* [8], who studied the current system using the pseudo-Maxwell molecule model. We found that the velocity distribution function predicted by this model differs qualitatively from those predicted by the inelastic hard sphere model.

ACKNOWLEDGMENTS

The authors thank J. A. Carrillo, C. Bizon, A. Santos, I. Gamba, Daniel I. Goldman, W. D. McCormick, and Harry L. Swinney for helpful discussion. This work was supported by the Engineering Research Program of the Office of Basic Energy Sciences of the Department of Energy (Grant No. DE-FG03-93ER14312).

APPENDIX A: DERIVATION OF EQ. (18)

The deviation from the MB distribution $g(c)$ is defined as in Eq. (17),

$$f^s_{(MD)}(c)=f_{MB}(c)[1+g(c)]. \tag{A1}$$

In the simulation, the number of particles in each bin is measured;

$$\int_{c_o}^{c_o+\Delta c} f^s_{(MD)}(c)dc=\int_{c_o}^{c_o+\Delta c}\frac{4}{\sqrt{\pi}}e^{-c^2}c^2[1+g(c)]dc, \tag{A2}$$

where the bin size Δc is assumed to be very small. It is possible to numerically solve for $g(c)$ from Eq. (A2), however, we get an approximate expression for $g(c)$ by assuming $g(c)$ is smooth in the scale of Δc;

$$\int_{c_o}^{c_o+\Delta c} e^{-c^2}c^2 g(c)dc\approx g\left(c_o+\frac{\Delta c}{2}\right)\int_{c_o}^{c_o+\Delta c} e^{-c^2}c^2\,dc. \tag{A3}$$

Equation (A2) can be read

$$g\left(c_o+\frac{\Delta c}{2}\right)\approx\frac{\displaystyle\int_{c_o}^{c_o+\Delta c} f^s_{(MD)}(c)dc}{\displaystyle\int_{c_o}^{c_o+\Delta c}\frac{4}{\sqrt{\pi}}e^{-c^2}c^2\,dc}-1. \tag{A4}$$

APPENDIX B: DERIVATION OF EQ. (21)

Starting from the definition of Sonine polynomials,

$$S^{(n)}_{1/2}(x)=\sum_{p=0}^{n}\frac{\left(\frac{1}{2}+n\right)!}{\left(\frac{1}{2}+p\right)!(n-p)!p!}(-x)^p, \tag{B1}$$

it can be shown that

$$c^{2k}=\sum_{p=0}^{k}\frac{(-1)^{k+p}\left(\frac{1}{2}+k\right)!k!}{\left(\frac{1}{2}+k-p\right)!p!}S^{(k-p)}_{1/2}(c^2). \tag{B2}$$

We assume the following Sonine polynomial expansion of the distribution function,

$$f^s_{(MD)}(c)=f_{MB}(c)\left[1+\sum_{p=2}^{\infty}a_p^{MD}S^{(p)}_{1/2}(c^2)\right]. \tag{B3}$$

Using Eqs. (B2) and (B3), $2k$th moment reads

$$\langle c^{2k}\rangle=\frac{(2k+1)!!}{2^k}\left[1+\sum_{p=0}^{k-2}(-1)^{k+p}\binom{k}{p}a_{k-p}^{MD}\right] \tag{B4}$$

or

$$a_k^{MD}=\frac{(-1)^k2^k}{(2k+1)!!}\langle c^{2k}\rangle+(-1)^{k+1}+\sum_{p=1}^{k-2}(-1)^{p+1}\binom{k}{p}a_{k-p}^{MD}, \tag{B5}$$

where $k>2$.

[1] H.M. Jaeger, S.R. Nagel, and R.P. Behringer, Rev. Mod. Phys. **68**, 1259 (1996).
[2] S.B. Savage and D.J. Jeffery, J. Fluid Mech. **110**, 255 (1981); P.K. Haff, *ibid.* **134**, 401 (1983); J.T. Jenkins and S.B. Savage, *ibid.* **130**, 187 (1983); C.K.K. Lun, S.B. Savage, D.J. Jeffery, and N. Chepurniy, *ibid.* **140**, 223 (1984); J.T. Jenkins and M.W. Richman, Arch. Ration. Mech. Anal. **87**, 355 (1985).
[3] S. Chapman and T.G. Cowling, *The Mathematical Theory of Non-uniform Gases* (Cambridge University Press, London, 1970).
[4] I. Goldhirsh, Chaos **9**, 659 (1999).
[5] T.P.C. van Noije and M.H. Ernst, Granular Matter **1**, 57 (1998).
[6] J.M. Montanero and A. Santos, Granular Matter **2**, 53 (2000).
[7] G.A. Bird, *Molecular Gas Dynamics and the Direct Simulation of Gas Flows* (Oxford University Press, New York, 1994).
[8] J.A. Carrillo, C. Cercignani, and I.M. Gamba, Phys. Rev. E **62**, 7700 (2000).
[9] A.V. Bobylev, J.A. Carrillo, and I.M. Gamba, J. Stat. Phys. **98**, 743 (2000).
[10] C. Bizon, M.D. Shattuck, J.B. Swift, W.D. McCormick, and H.L. Swinney, Phys. Rev. Lett. **80**, 57 (1998).
[11] D.L. Ermak and J.A. McCammon, J. Chem. Phys. **69**, 1352 (1978).
[12] D.R.M. Williams and F.C. MacKintosh, Phys. Rev. E **54**, R9 (1996).
[13] R. Balescu, *Equilibrium and Nonequilibrium Statistical Mechanics* (Wiley, New York, 1975).
[14] D. Burnett, Proc. London Math. Soc. **2**, 39, 385 (1935).
[15] A. Goldshtein and M. Shapiro, J. Fluid Mech. **282**, 75 (1995).
[16] J.A. Carrillo (private communication).
[17] M.R. Swift, M. Boamfa, S.J. Cornell, and A. Maritan, Phys. Rev. Lett. **80**, 4410 (1998); J.A.G. Orza, R. Brito, T.P.C. van Noije, and M.H. Ernst, Int. J. Mod. Phys. C **8**, 953 (1998).
[18] T.P.C. van Noije, M.H. Ernst, E. Trizac, and I. Pagonabarraga, Phys. Rev. E **59**, 4326 (1999).
[19] W. Losert, D.G.W. Cooper, J. Delour, A. Kudrolli, and J.P. Gollub, Chaos **9**, 682 (1999).
[20] E. Trizac (private communication).
[21] R. Soto and M. Mareschal, Phys. Rev. E **63**, 041303 (2001).